A NOVEL SLOTTED HELIX SLOW-WAVE STRUCTURE FOR MILLIMETER-WAVE TRAVELING-WAVE TUBE

Luwei Liu, Yanyu Wei*, Jin Xu, Zhigang Lu, Hairong Yin, Lingna Yue, Huarong Gong, Guoqing Zhao, Zhaoyun Duan, Wenxiang Wang, and Yubin Gong

National Key Laboratory of Science and Technology on Vacuum Electronics, University of Electronic Science and Technology of China, Chengdu 610054, China

Abstract—A novel slotted helix slow-wave structure (SWS) is proposed to develop high power, wide-bandwidth, high reliability millimeter-wave traveling-wave tube (TWT). This structure, which can improve the heat dissipation capability of the helix SWS, evolves from conventional helix SWS with three parallel rows of rectangular slots made in the outside of the helix. In this paper, thermal stress analysis, the electromagnetic characteristics and the beam-wave interaction of this structure are investigated. The conclusions of this paper will be a great help for the design of millimeter-wave traveling-wave tube.

1. INTRODUCTION

Millimeter-wave radiation sources with high power, wide-bandwidth, and high efficiency are attractive for many applications, such as high-date-rate communications, high-resolution radar, and space applications [1–8]. Helix TWT is one of the most important millimeter-wave vacuum amplifiers due to its outstanding combined performances in bandwidth, power capacity, and electronic efficiency. But because of its high thermal resistance in the helix SWS, the average-power limits of the conventional millimeter-wave helix TWT have long been quite well known [9, 10]. Moreover, the high temperature produced by electron beam interception and RF loss could make the helix deform, which seriously changes the dispersion characteristics of the millimeter-wave helix SWS [11, 12].

In order to improve the heat dissipation capability of the millimeter-wave helix TWT, Diamond support rod [13, 14], brazed-helix technology [15–19] have been used for high power millimeter-wave TWT. At present known, Diamond has the highest thermal conductivity, but it has been founded that the overall thermal resistance from the helix to the shell significantly increased for the diamond support rod design [20]. Brazed-helix technology used for TWT mainly includes sputter brazing method and diffusion brazing method [21]. It offers lower thermal resistance of the helix-rod interface and the rod-shell interface than non-brazed helix technology, thus ensuring better thermal evacuation capability for transmitting high power levels. While sputter brazing method has some problems, such as the redundant solders are not easy to be completely cleared [21] and the sputter brazed-helix SWS could generate thermal stress and deformation, and lack the mechanical strength [22]. The helix SWS is assembled using diffusion brazing method without any solder, but the contact width between helix tape and support rod is smaller than the width of the support rod, which also limit the heat dissipation out of the helix SWS.

Thus how to circumvent these limitations and further improve the heat dissipation capability of the helix SWS is an interesting and important question for exploring high power, wide-bandwidth millimeter-wave TWT. Fortunately, a novel slotted helix SWS plus diffusion brazing method, which can reduce the interface resistance and increase the contact area between helix tape and support rod, is now proposed by Wei et al. [23]. The preliminary thermal analysis shows that the novel slotted helix SWS has better heat dissipation capability than that of the conventional helix SWS [24]. The processing method of this new structure will be discussed in this paper. Thermal stress analysis, high-frequency characteristics and the beam-wave interaction of the novel structure are calculated using software ANSYS [25] and three-dimensional (3-D) high-frequency electromagnetic simulation software (HFSS) [26] and the PIC solver in CST Particle Studio [27].

This paper is organized in the following manner. A brief introduction is presented in Section 1. The mode of the novel slotted millimeter-wave helix SWS is described in Section 2. The thermal analysis model of the novel slotted helix SWS is constructed in Section 3. High-frequency characteristics are calculated in Section 4. The simulation results of the beam-wave interaction of the novel structure operating in the Ka-band are given in Section 5. A brief summary is given in Section 6.
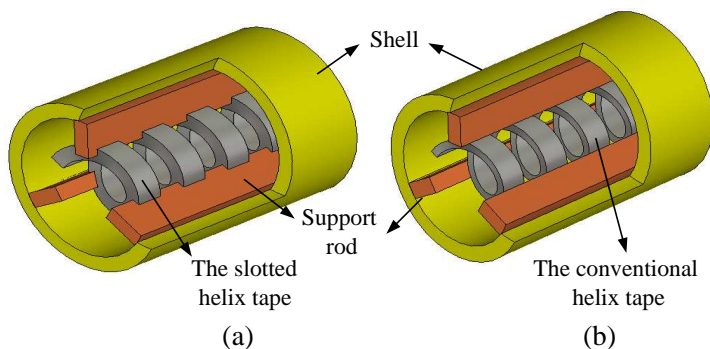
Figure 1. (a) Cutaway view of the novel slotted helix SWS. (b) Cutaway view of the conventional helix SWS.

2. THE NOVEL SLOTTED MILLIMETER-WAVE SLOW-WAVE STRUCTURE DESIGN

2.1. The Novel Slotted Helix SWS Description

Figure 1(a) shows the three-dimensional model of the novel slotted helix SWS, which consists of a slotted helix tape, three Beryllia support rods and a stainless steel shell. This novel structure is derived from the idea of increasing thickness of conventional helix tape as shown in Figure 1(b), and then three parallel rows of rectangular slots are made in the outside of the helix. The three rows of rectangular slots are lined in parallel with the central axis of the helix and spaced 120° apart around the helix. The rectangular support rods are inserted into the slots tightly within the shell. The slots can not only increase the contact area between the helix tape and support rods, but also can enhance the stability of the helix SWS. Based on the novel slotted helix SWS, high power, and high reliability millimeter wave helix TWTs are expected.

Figure 2 shows the dimensional parameters of the novel slotted helix SWS. Where, a is the inner radius of the helix tape, b is the thickness of the helix tape, c is the inner radius of the shell, d is the width of the support rods, g is the outer radius of the shell, h is the depth of the slot, p is the pitch of the novel helix SWS, and w is the width of the helix tape. The typical optimized parameters of structure are listed in Table 1.
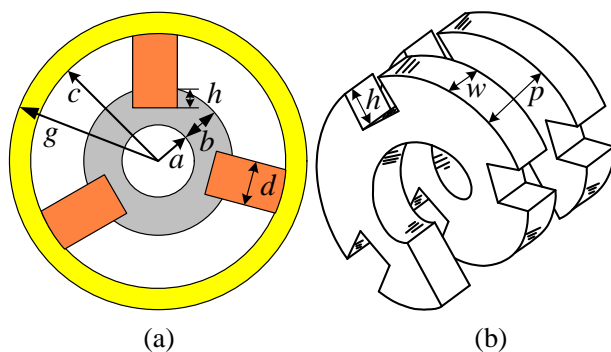
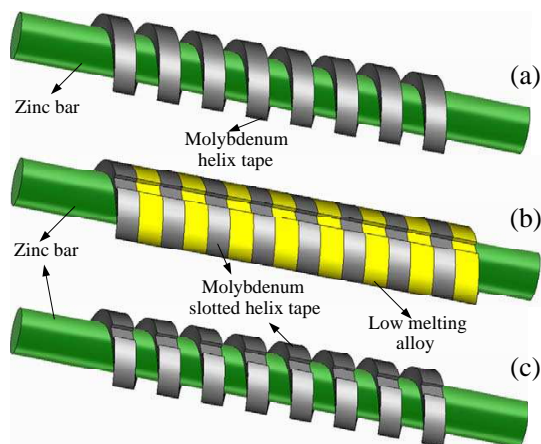**Figure 2.** Dimensional parameters of the novel slotted helix SWS.

Figure 3. The processing method of the novel slotted helix SWS.

Table 1. Optimized parameters of structure.

Parameter	a/b	c/b	d/b	g/b	h/b	p/w	w/b
Value/mm	1.5	5	1	6.25	0.5	2	0.8

2.2. The Processing Method of the Novel Slotted Helix Structure

Figure 3 shows the processing method of the novel slotted helix SWS. After the molybdenum helix tape is wrapped around the Zinc bar, as shown in Figure 3(a), low melting alloy such as Indium alloy is filled in the interspaces of the helix tape, as shown in Figure 3(b),

which will help the helix tape resist deformation during the process for machining the slots. After the slot processing is completed, Zinc bar with the slotted helix tape and low melting alloy is placed in the high temperature furnace to get rid of the low melting alloy and then the slotted helix tape is produced, as shown in Figure 3(c). After that, the exterior surface of the helix tape and the inner surface of the shell are plated with a copper film. And then, the novel helix SWS is assembled by the hot-insertion method to provide enough pressure. At last, the novel slotted helix SWS is heated at high temperature in a hydrogen furnace for diffusion brazing. Under this processing method, all the components of the slotted helix SWS are brazed together.

3. THERMAL STRESS ANALYSIS OF THE NOVEL HELIX SWS

Three methods including theoretical analysis [28, 29], experiment test [30–32], and numerical simulation [11, 12, 33–36] can be used to analyze thermal characteristics of the helix SWS. It has been proved that simulation results show very good agreement with the experimental and calculated data [11, 32]. Because numerical simulation can get detailed three dimensional temperature distributions of a helix SWS, this method is employed in this paper to accurately calculate the thermal characteristics of the helix SWS.

The thermal stress characteristics of the novel helix SWS is simulated by software ANSYS. Steady state thermal stress analysis has been used to simulate the circuit's response in this paper. The thermal stress analysis belongs to multidiscipline coupled-field analysis. The direct coupling method and the indirect coupling method provided by ANSYS are the two kinds of coupling field analysis methods [25]. The thermal stress analysis of the novel helix SWS is calculated by indirect coupling method in this paper.

The last ten helix turns of the novel slow-wave circuit is selected to perform the thermal stress analysis, where the largest temperature gradient has been found in experiments, and therefore the biggest thermal deformation will occur in this area. The simulation model includes a novel rectangular copper-plated helix tape made of Molybdenum, three rectangular support rods made of Beryllia, and a copper-plated stainless steel shell. Because the novel helix SWS is enveloped in vacuum, there is no convection, and the effect of radiation from helix can be neglected [12], thus the heat is transferred only by conduction from the helix through the support rods to the metal shell. The thermal conductivities of the materials are only needed in the thermal analysis, and they are all temperature

dependent [29]. Thermal contact resistance of the brazed-helix SWS is set as $0.056°C \cdot cm^2/W$, which is given by Raytheon Company [37]. The convection coefficient of the outer surface of the shell is set as $2000\,W/m^2 \cdot °C$, which is suitable for brazed helix SWS suggested by Qinqun Zhao [35]. We suppose the ambient temperature is $30°C$. A simulated thermal flux is applied to the inner surface of the helix to represent electron bombardment and RF loss.

The results of the steady state thermal analysis are used as a thermal load condition for ANSYS static structure analysis. The material properties necessary for the stress analysis are Young's modulus, the Poisson ratio, and the thermal expansion coefficient. Because the shell is brazed in the pole, the outer surface of the shell is set zero displacement boundary condition. Here, in order to describe the superiority of the novel slotted helix SWS, the thermal stress distributions of the conventional helix SWS are also calculated as a comparison for the same conditions except the thickness of the helix tape a/b is equal to 3.

In the process of thermal stress analysis, hexahedral element Solid90 and hexahedral mesh are adopted for thermal analysis, and then the thermal analysis element is replaced by the structure analysis element Solid186. The whole model produces a total of 20707 elements and 111270 nodes after meshing the model into elements. The platform used for the calculation is a personal computer with Inter(R) core(TM) i7-2600 3.4 G CPU with 12 GB memory. The CPU time is approximate 2 min for a single thermal stress analysis.

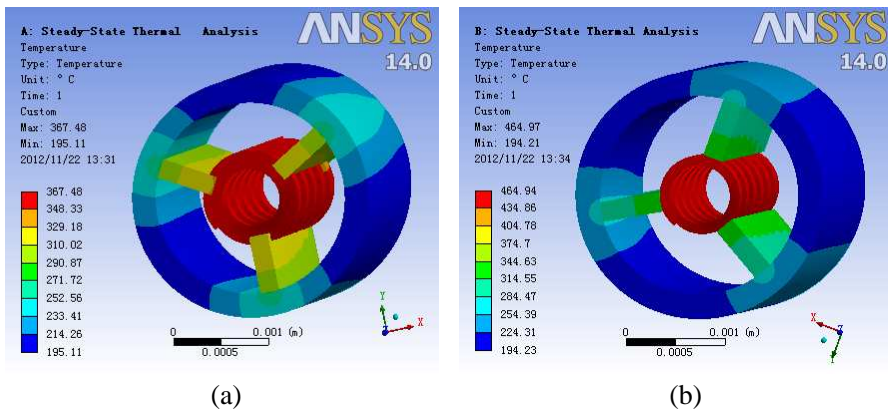Figure 4 shows temperature distributions of the novel and

(a)   (b)

Figure 4. (a) Temperature distribution of the novel helix SWS. (b) Temperature distribution of the conventional helix SWS.

conventional helix SWS when the total dissipation power is 22 W.
As can be seen, the temperature of the novel helix tape is smaller
than that of conventional one in the same cooling conditions. That
is to say, the heat generated by the dissipation power can be easily
conducted out from the novel structure. Figure 5 shows the thermal
deformation distributions corresponding to Figure 4 respectively (50
times enlarged). As can be seen from the two figures, the thermal
stress makes the helix tape concave at the positions contacting with
the support rods and convex at the part between two adjacent support
rods, and the maximum deformation point in the helix tape is also
between two adjacent support rods. Meanwhile, the values of the
maximum deformation have already marked in the Figure 5. And
the maximum deformation of the conventional helix SWS is almost 2.6
times than that of the novel helix SWS, which shows that the novel
structure is more reliable. In the ANSYS model, a uniform heat flux is
applied along the inner surface of the helix. As this flux is varied, the
different thermal stress distributions of the helix SWS are obtained, as
shown in Figure 6.

In order to study the thermal stress characteristic of the novel
slotted helix SWS more specifically, the influences of the thickness of
the slotted helix tape on the novel helix temperature and the maximum
deformation of the novel helix SWS are investigated. Here, only the
thickness of the helix tape changes without changing other parameters.
Figure 7(a) shows the relationship between helix temperature and
dissipation power at different helix thickness. Figure 7(b) displays the
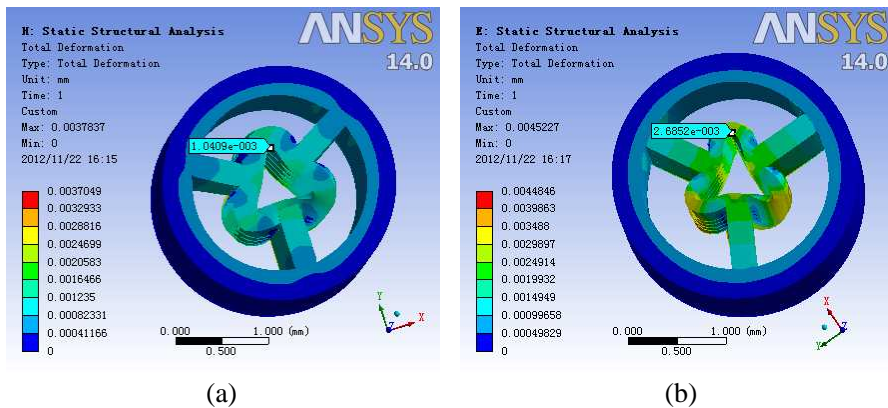changes in maximum deformation with dissipation power at different

(a)   (b)

Figure 5. (a) Thermal stress distribution of the novel helix SWS.
(b) Thermal stress distribution of the conventional helix SWS.

helix thickness. From the two plots, it is obvious that the helix thickness has a pronounced effect on the temperature and thermal deformation of the slotted helix SWS. When the thickness of the slotted helix tape is doubled and the helix SWS dissipate the same power between 4 W and 28 W, the temperature of the helix tape is reduced by 15%~22%, and simultaneously the maximum thermal deformation of the helix tape is reduced by 48% ∼ 51%. Therefore, increasing the thickness of the helix tape can not only improve the heat capacity of the helix SWS, but also can reduce the thermal deformation of the helix
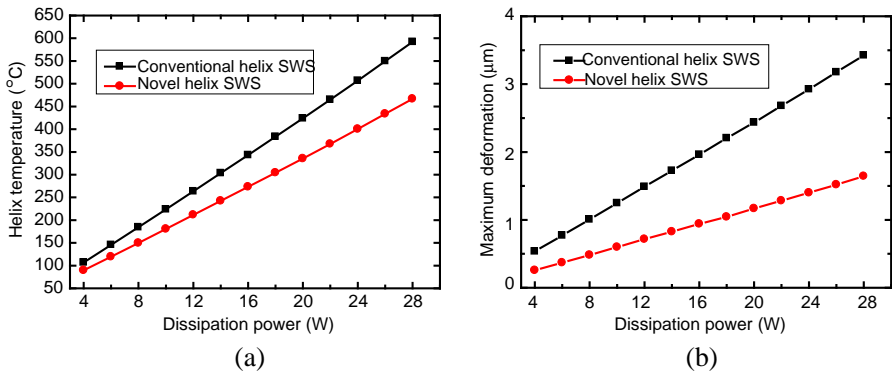

Figure 6. (a) Heat dissipation capability comparison for the conventional and the novel helix SWS. (b) The maximum thermal deformation comparison for the conventional and the novel helix SWS.
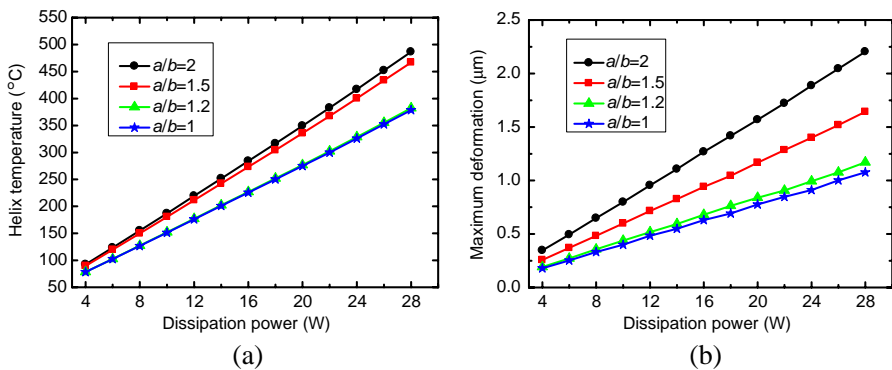

Figure 7. (a) Effect of the helix tape thickness b on the helix temperature. (b) Effect of the helix tape thickness b on the maximum deformation of the novel helix SWS.

SWS effectively, which is very important for high power millimeter-wave helix TWT [38].

4. ELECTROMAGNETIC PROPERTIES

The high-frequency properties of the slotted helix SWS are calculated by the eigenmode solver with master and slave boundary condition [39] in the 3-D electromagnetic simulation software Ansoft HFSS [26]. The optimized dimensional parameter values of the slotted helix SWS are presented in Table 1. Figure 8 shows Brillouin diagram of the slotted helix SWS, which is the same as that of the conventional helix SWS, so the novel helix slow-wave circuit is also a fundamental forward wave circuit and the electron beam interacts with the zero space harmonic. As shown in Figure 8, mode 1 ($n = 0$) and mode 1 ($n = -1$) is zero and minus-first space harmonic for the fundamental mode, while mode 2 ($n = -1$) and mode 2 ($n = -2$) is minus-first and minus-second space harmonic for the second mode. Figure 9 shows comparison of dispersion characteristics and interaction impedance of the fundamental mode at the zero space harmonic for the conventional and the novel slotted helix SWS. Here, the dimensional parameters of the conventional helix SWS are the same as described in Section 3. It shows that the normalized phase velocity of the novel helix SWS is lower than that of the conventional helix SWS, which shows that the novel structure has lower working voltage, and thus the risk of backward wave oscillation may be reduced. In addition, the dispersion curves of the two helix SWS are nearly parallel, although the interaction impedance of the novel helix SWS is smaller than
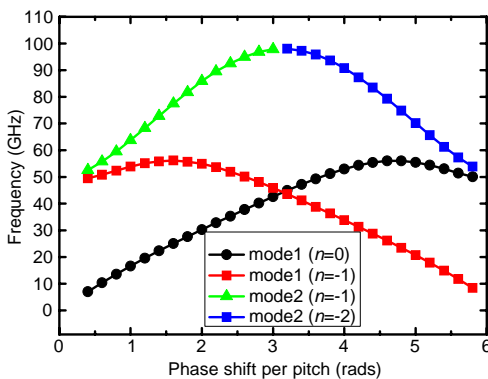

Figure 8. Brillouin diagram of the slotted helix SWS

that of the conventional helix SWS, we can increase the length of the interaction circuit to obtain higher power, wide-bandwidth, high reliability millimeter-wave traveling-wave tube.

In order to study the high-frequency characteristics of the novel slotted helix SWS further, the influences of the thickness of the slotted helix tape on dispersion relation and interaction impedance are investigated. It is shown in Figure 10 that, with the helix tape thickness increase, normalized phase velocity decreases, and
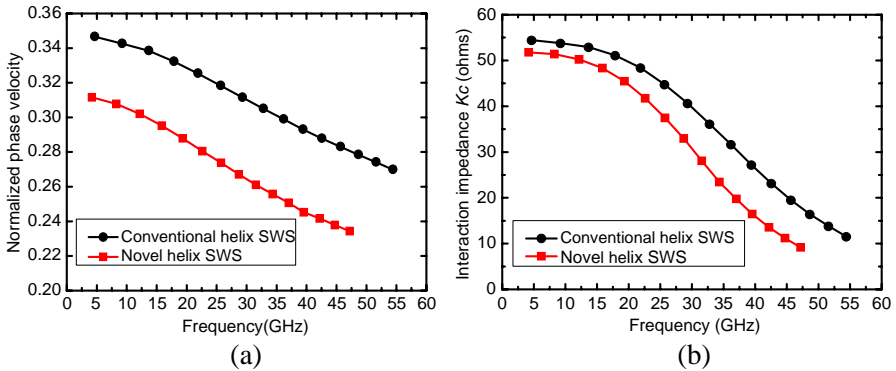

Figure 9. (a) Comparison of dispersion characteristics for the conventional and the novel slotted helix SWS. (b) Comparison of the interaction impedance for the conventional and the novel slotted helix SWS.
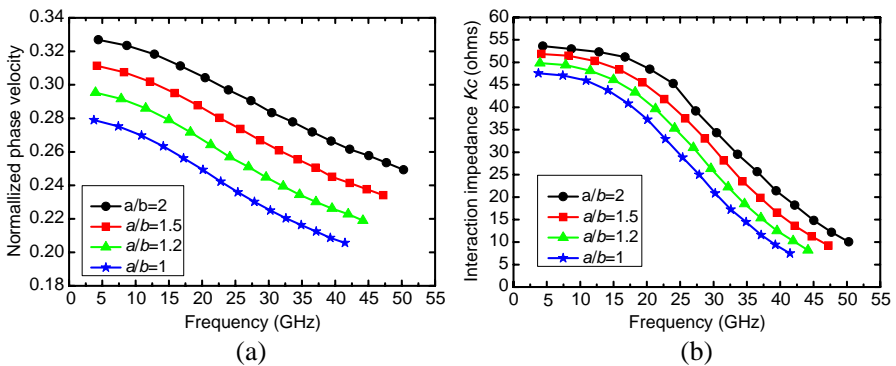

Figure 10. (a) Effect of the helix thickness b on the normalized phase velocity. (b) Effect of the helix thickness b on the interaction impedance.

the interaction impedance also decreases noticeably. But we should choose proper helix tape dimensions considering both passband and the interaction impedance.

5. BEAM WAVE INTERACTION SIMULATION

In this section, a fully three-dimensional, time-dependent model for a novel slotted helix TWT operating in the Ka-band is designed. The beam-wave interaction simulations are carried out by using the PIC solver in CST Particle Studio [27] to substantiate the amplification capability of the TWT. The parameters for PIC simulation are as follows: $a/b = 1.5$, $c/b = 4$, $d/b = 1$, $h/b = 0.5$, $p/w = 2$, $w/b = 0.18$. Reflections caused by circuit discontinuities such as the mismatches between the input/output couplers can cause reflection oscillation, while the backward wave, especially minus-first space harmonic of the fundamental mode interacting with the electron beam can cause BWO [40, 41]. In order to obtain large gain, the whole interaction circuit is divided into two section with sever, and two concentrated attenuators are used in the interaction circuit to suppress these oscillation.

In the simulation, the beam filling factor is set as 0.65 with a voltage of 18.45 kV and a current of 0.2 A. In addition, a uniform longitudinal magnetic field of 0.35 T is used here to confine the electron beam. Then, we apply an input signal with a power of 72.2 mW. The boundary is specified as copper with the effective conductivity of 5.8×10^7 S/m. Moreover, the CPU (i7-2600 3.4 G CPU with 12 GB) time is approximately 50 h for a signal frequency with 8-ns calculation.
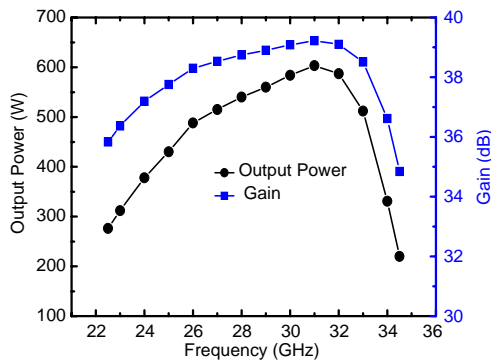

Figure 11. Simulation results of the output power and total gain versus frequency of the novel slotted helix TWT.

Figure 11 shows the output power versus the driving frequencies from 22.5 GHz to 34.5 GHz, where the corresponding gain is also given. The dots are the simulation values for each operating frequency, and the line is a B-spline fit curve. It shows that the CW output power exceeds 500 W in the frequency range of 27 GHz to 33 GHz, corresponding to the gain of over 38.5 dB. Especially, gain changes only 0.7 dB across the 6-GHz bandwidth, which can satisfy many applications, including space communication. Meanwhile, the instantaneous 3-dB bandwidth of this TWT ranges from 23 GHz to 34 GHz.

6. CONCLUSION

In conclusion, a novel slotted helix SWS for millimeter-wave TWT has been investigated in this paper. The thermal analysis, electromagnetic and beam-wave interaction of the novel structure are simulated. It has been found that the novel slotted helix SWS has similar spectral response as a conventional helix SWS. Meanwhile, it has some unique advantages, including higher heat capacity, smaller thermal deformation. Therefore, it is a promising slow-wave structure for developing high power, wide-bandwidth, high reliability millimeter-wave radiation sources. Future work will be concentrated on the experimental research of this novel slotted helix TWT.

ACKNOWLEDGMENT

REFERENCES

1. Safier, P. N., V. Dronov, T. M. Antonsen, J. X. Qiu, B. G. Danly, and B. Levush, "From frequency-domain physics-based simulation to time-domain modeling of traveling-wave tube amplifiers for high data-rate communication applications," *IEEE Trans. Microw. Theory Tech.*, Vol. 54, No. 10, 3605–3615, Oct. 2006.

2. Qiu, J. X., B. Levush, J. Pasour, A. Katz, C. M. Armstrong, D. R. Whaley, J. Tucek, K. Kreischer, and D. Gallagher, "Vacuum tube amplifiers," *IEEE Microw. Mag.*, Vol. 10, No. 7, 38–51, Dec. 2009.

3. Komm, D. S., R. T. Benton, H. C. Limburg, W. L. Menninger, and X. L. Zhai, "Advances in space TWT efficiencies," *IEEE Trans. Electron Devices*, Vol. 48, No. 1, 174–176, Jan. 2001.

4. Kesari, V. and J. P. Keshari, "Analysis of a circular waveguide loaded with dielectric and metal discs," *Progress In Electromagnetics Research*, Vol. 111, 253–269, 2011.

5. Li, Z., J. H. Wang, F. Li, Z. Zhang, and M. E. Chen, "A new insight into the radiation mechanism of fast and slow traveling waves," *Journal of Electromagnetic Waves and Applications*, Vol. 25, No. 13, 1874–1885, 2011.

6. Liu, Y., J. Xu, Y. Wei, X. Xu, F. Shen, M. Huang, T. Tang, W. Wang, Y. Gong, and J. Feng, "Design of a V-band high-power sheet-beam coupled-cavity traveling-wave tube," *Progress In Electromagnetics Research*, Vol. 123, 31–45, 2012.

7. Shen, F., Y.-Y. Wei, X. Xu, Y. Liu, H.-R. Yin, Y.-B. Gong, and W.-X. Wang, "140-GHz V-shaped microstrip meander-line traveling-wave tube," *Journal of Electromagnetic Waves and Applications*, Vol. 26, No. 1, 89–98, 2012.

8. Hou, Y., J. Xu, H.-R. Yin, Y.-Y. Wei, L.-N. Yue, G.-Q. Zhao, and Y.-B. Gong, "Equivalent circuit analysis of ridge-loaded folded-waveguide slow-wave structures for millimeter-wave traveling-wave tubes," *Progress In Electromagnetics Research*, Vol. 129, 215–229, 2012.

9. Han, Y., Y. W. Liu, Y. G. Ding, and P. K. Liu, "Study on the thermal interface resistance of the helix slow-wave structure," *Acta Physica Sinica*, Vol. 58, No. 3, 1806–1811, Mar. 2009.

10. Fleury, G., C. Deville, and J. C. Kuntzmann, "Average power limits of brazed-helix TWT's," *1980 International Electron Devices Meeting Technical Digest*, Vol. 26, 806–809, 1980.

11. Yao, L. M., Z. H. Yang, Z. S. Huo, X. F. Zhu, and B. Lin, "Simulation of thermal characteristics for helical slow-wave circuit of TWT," *International Conference on Microwave and Millimeter Wave Technology*, 1–3, 2007.

12. Yan, S. M., L. M. Yao, and Z. H. Yang, "Effect of thermal strain in helical slow-wave circuit on TWT cold-test characteristics," *IEEE Trans. Electron Devices*, Vol. 55, No. 8, 2278–2281, Aug. 2008.

13. Xie, K. J., "CAD Diamond rod and its application in the high power TWT," *The 25th Infrared and Millimeter Wave Conference*, 343–344, 2000.

14. Dayton, J. A., G. T. Mearini, H. Chen, and C. L. Kory, "Diamonded-studded helical traveling wave tube," *IEEE Trans.*

Electron Devices, Vol. 52, No. 5, 695–701, May 2005.

15. Fleury, G., J. C. Kuntzmann, and P. Lafuma, "High-power brazed-helix telecommunications TWT's," *1977 International Electron Devices Meeting Technical Digest*, Vol. 23, 116–119, 1977.

16. Henry, D., N. Sntonja, and S. Wartski, "Brazed-helix technology for 30 GHz power TWTs," *1986 International Electron Devices Meeting Technical Digest*, 505–507, 1986.

17. Wartski, S., D. Henry, and N. Santonjia, "Development of a brazed-helix TWT for future Ka-band earth stations delivering 200 W in the band 27.5–30 GHz," *1988 International Electron Devices Meeting Technical Digest*, 366–369, 1988.

18. Gong, Y., Y. Wei, W. Wang, and Z. Duan, "Analysis of a novel brazed helix tape slow wave structure with high power capability," *30th IEEE International Conference on Plasma Science*, 177, 2003.

19. Lee, J. S. and C. Everleigh, "High power CW BeO block brazed copper helix TWT," *Proc. IEEE International Vacuum Electronics Conference*, 185–186, 2006.

20. Toups, C. E. and D. K. Yamadam, "Thermal/structural analysis of diamond supported helices," *AIAA 11th Communication Satellite Systems Conference*, 605–608, 1986.

21. Han, Y., Y. W. Liu, Y. G. Ding, and P. K. Liu, "Improvement of heat dissipation capability of slow-wave structure using two assembling methods," *IEEE Electron Devices Letters*, Vol. 29, No. 8, 955–956, Aug. 2008.

22. TaKahashi, M., T. Yamaguchi, H. Hashimoto, T. Konishi, and H. Sato, "Non-brazed helix TWT attained 3 kW output at C-band and 600 W at Ku-band," *1986 International Electron Devices Meeting Technical Digest*, 167–170, 1986.

23. Wei, Y. Y., L. W. Liu, Y. B. Gong, X. Xu, H. R. Yin, L. N. Yue, Y. Liu, J. Xu, and W. X. Wang, "Helical slow-wave structure," USA Patent Application, No. 13/345, 121, Jan. 6, 2012.

24. Liu, L., Y. Wei, X. Xu, F. Shen, G. Zhao, M. Huang, T. Tang, W. X. Wang, and Y. Gong, "A novel helical slow-wave structure for millimeter wave traveling wave tube," *5th Global Symposium on Millimeter Waves Conference*, 312–315, 2012.

25. ANSYS, Inc., "Analysis guide," Release 14.0, 2012.

26. Ansoft Corp., "Ansoft HFSS user's reference," Online Available: http://www.ansoft.com.cn/.

27. CST Corp., "CST PS tutorials," Online Available: http://www.cst-china.cn/.

28. Lucken, J. A., "Some aspects of circuits power dissipation in high power CW helix traveling-wave tubes, Part I: General theory," *IEEE Trans. Electron Devices*, Vol. 16, No. 9, 813–820, Sep. 1969.

29. Crivello, R. and R. W. Grow, "Thermal analysis of PPM-focused rod-supported TWT helix structures," *IEEE Trans. Electron Devices*, Vol. 35, No. 10, 1701–1720, Oct. 1988.

30. Sauseng, O., A. E. Mauoly, and A. Hall, "Thermal properties and power capability of helix structures for millimeter waves," *1978 International Electron Devices Meeting Technical Digest*, Vol. 24, 534–537, 1978.

31. Han, Y., Y. Liu, Y. Ding, and P. Liu, "An evaluation of heat dissipation capability of slow-wave structures," *IEEE Trans. Electron Devices*, Vol. 54, No. 6, 1562–1565, Jun. 2007.

32. Han, Y., Y. Liu, Y. Ding, P. Liu, and C. Lu, "Thermal analysis of a helix TWT slow-wave structure," *IEEE Trans. Electron Devices*, Vol. 55, No. 5, 1269–1272, May 2008.

33. Bartos, K. F., E. B. Fite, K. A. Shalkhauser, and G. R. Sharp, "A three-dimensional finite-element thermal/mechanical analytical technique for high-performance traveling wave tubes," NASA Technical Paper 3081, 1–14, 1991.

34. Rocci, P. J., "Thermal-structural reliability assessment of helix TWT interaction circuit using finite element analysis," *Proc. Aerosp. Electron. Conf.*, 731–737, 1993.

35. Zhao, X. Q., G. X. Zhang, and X. H. Sun, " The analysis and ANSYS simulation for the thermal condition of pulse helix TWT," *Acta Electronica Sinica*, Vol. 32, No. 6, 1029–1032, 2004.

36. Han, Y., Y. Liu, Y. Ding, and P. Liu, "Reliability analysis of thermal conduction of slow-wave structures assembled with different methods," *IEEE Trans. Electron Devices*, Vol. 9, No. 2, 265–268, May 2009.

37. Harper, R. and M. P. Puri, "Heat transfer and power capabilities of EFH helix TWT's," *1986 International Electron Devices Meeting Technical Digest*, 498–500, 1986.

38. Chong, C. K., J. A. Davis, R. H. Le Borgne, M. L. Ramay, R. J. Stolz, R. N. Tamashiro, J. P. Vaszari, and X. Zhai, "Development of high-power Ka-band and Q-band helix-TWTs," *IEEE Trans. Electron Devices*, Vol. 52, No. 5, 653–659, May 2005.

39. Booske, J. H., M. C. Converse, C. L. Kory, C. T. Chevalier, D. A. Gallagher, K. E. Kreischer, V. O. Heinen, and S. Bhattacharjee, "Accurate parametric modeling of folded waveguide circuits for millimeter wave traveling wave tubes,"

IEEE Trans. Electron Devices, Vol. 52, No. 5, 685–694, May 2005.

40. Antonsen, Jr., T. M., P. Safier, D. P. Chernin, and B. Levush, "Stability of traveling-wave amplifiers with reflections," *IEEE Trans. on Plasma Science*, Vol. 30, No. 3, 1089–1107, Jun. 2002.

41. Chernin, D., T. M. Antonsen, Jr., and B. Levush, "'Power holes' and nonlinear forward and backward wave gain competition in helix traveling-wave tubes," *IEEE Trans. Electron Devices*, Vol. 50, No. 12, 2540–2547, Dec. 2003.